Digest of Tech. Papers The 8th Conf. (1976 International) on Solid State Devices, Tokyo

A-6-5

Analysis of Silicon Solar Cell with Multi-Layer Structure

Takeshi Matsushita, Masayuki Miyake*, and Takayoshi Mamine

Semiconductor Development Division and *Semiconductor Production , SONY Corporation

4-14-1 Asahi, Atsugi 243, Kanagawa, Japan

A new class of silicon solar cell which has $p^+npn{-}{-}pn^+$ multi-layer structure has been developed[1]. In this cell, the p- and n-layers are paralleled to the surface, and electrodes are attached to the top p_1^+ layer and the bottom n_m^+ layer as shown in Fig. 1. The operation of this solar cell is as follows. When the light generates holes and electrons, these carriers are separated by electric fields in each p-n junction and holes are trapped by the p layers and electrons by the n layers. Therefore, by these trapped carriers, each junction becomes forward self-baised condition and the impeadance of each junction becomes low and current can flow across the junction. Now we consider the case that a hole is generated within n_4 layer which is at a long distance from the top p_1^+ layer. The generated hole diffuses to the junction J_3 and is collected into the p_3 layer and becomes a majority carrier. As soon as it crosses the junction J_3, another hole is injected through the junction J_2 into the n_2 layer and at last collected into the p_1^+ layer. This mechanism means that the diffusion velocity of the photo-generated minority carrier increases and the effective recombination rate is reduced. Thus, the minority carrier diffusion length of the multi-layer solar cell is effectively longer than that of the conventional solar cells, and the maximum conversion efficiency of the multi-layer solar cell approaches 21 % theoretically at AM 0.

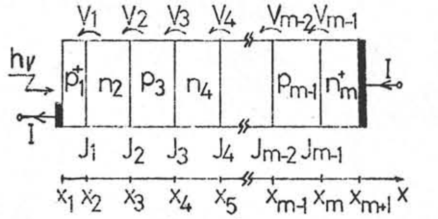

Figure 1

	N_i cm^{-3}	D_i $cm^2 sec^{-1}$	τ_i μsec^{-1}	L_i μm	S $cm \cdot sec^{-1}$
p_1^+	5×10^{20}	.5	1×10^{-3}	.22	10^3
n_2	1×10^{17}	8.	33.	163.	—
p_3	1×10^{17}	20.	70.	374.	—
⋮	⋮	⋮	⋮	⋮	
n_m^+	1×10^{19}	2.	1×10^{-1}	45	10^5

Table 1

The multi-layer silicon solar cell is theoretically analyzed at AM 0 by a simplified "one dimentional" first order solar cell model, which assumes a straightforward superposition of a constant optically generated current with the diffusion model for a forward biased diode and neglects depletion region recombination, high injection and drift currents.

In each layer of the multi-layer solar cell, the continuity equations for the excess minority carrier concentration in the steady-state condition are expressed by

$$D_i\left(d^2 f_i/dx^2\right) - f_i/\tau_i = -\int_0^{\lambda_G} \alpha(\lambda)\, N(\lambda)\, \exp\left\{-\alpha(\lambda)x\right\} d\lambda, \quad (i=1,\ 2,\ \ldots,\ m) \tag{1}$$

where D_i, τ_i and f_i are the minority carrier diffusion constant, the minority lifetime and the excess minority carrier concentration of the layer i, respectively; and λ, λ_G, $\alpha(\lambda)$ and $N(\lambda)$ are the wavelength, the upper limit of the useful wavelength, the absorption coefficient and the number of incident photons, respectively.

The above equations can be solved with the following boundary conditions (2)-(5) and the terminal voltage of the solar cell can be calculated by the following equations (6) and (7).

$$D_1 \left.\frac{df_1}{dx}\right|_{x_1} = S_n f_1\Big|_{x_1} \quad (2) \qquad D_m \left.\frac{df_m}{dx}\right|_{x_{m+1}} = S_p f_m\Big|_{x_{m+1}} \quad (3) \qquad (-1)^{i-1} qD_i \left.\frac{df_i}{dx}\right|_{x_{i+1}} + (-1)^i qD_{i+1} \left.\frac{df_{i+1}}{dx}\right|_{x_{i+1}} = I \quad (4)$$

$$\left.\frac{f_i}{f_{i+1}}\right|_{x_{i+1}} = \frac{N_{i+1}}{N_i} \quad (5) \qquad f_i\Big|_{x_{i+1}} = \frac{n_i^2}{N_i}\left\{\exp\left[(-1)^{i-1} qV_i/kT\right] - 1\right\} \quad (6) \qquad V = \sum_{i=1}^{m-1} V_i \quad (7)$$

Where s_n, s_p, n_i, N_i and V_i are the electron surface recombination velocity, the hole surface recombination velocity, the intrinsic carrier concentration, the impurity concentration of the layer i and the self-biased voltage of the junction J_i, respectively; and I and V are the terminal current and voltage, respectively.

Table 1 shows the constant which are assumed in the multi-layer solar cell. Then, the calculated energy band diagram of the six layer solar cell under short-circuit condition is shown in Fig.2. It is understood by Fig.2 that photo-generated holes tend to flow to the top p_1^+ layer and electrons to the bottom n_1^+ layer within the solar cell, because the hole potential energy of the p layers becomes lower in the order, p_5, p_3, p_1^+ and the electron potential energy of the n layers in the order, n_2, n_4, n_6^+. Figure 3 shows the distributions of the minority carrier current density of the multi-layer and the back-surface field p^+nn^+ solar cells, in which the same constants as Table 1 are used. The current density of multi-layer solar cell is larger than that of the p^+nn^+ solar cell, which means that the multi-layer solar cell can reduce the series resistance loss as compared with the p^+nn^+ solar cells.

Figure 4 shows the collection efficiencies of the multi-layer, the p^+nn^+ and the conventional p^+n solar cells, where each solar cell thickness is 120 μm. The collection efficiencies of the multi-layer solar cell is higher than those of the p^+nn^+ and p^+n solar cells in the longer wavelength. In order to visualize this phenomenon, the quantum photo responces of the long wavelength (α = 10/cm) are shown in Fig.5 as a function of the solar cell thickness in the case of L_p=L_n=50 μm, which shows that the effective minority carrier diffusion length of the multi-layer solar cell is longer. Figure 6 shows the conversion efficiencies of the solar cells calculated by using the constants of Table 1 as a function of solar cell thickness. As shown in Fig.6, the maximum efficiency of the multi-layer solar cell is about 21 % at AM 0, which is still higher than that of the p^+nn^+solar cells having high efficiency previously described[2].

References

(1) T. Matsushita and T. Mamine, 1975 IEDM Technical Digest, (1975) p.353.

(2) K. G. Fossum, 1975 IEDM Technical Digest, (1975) p.339.

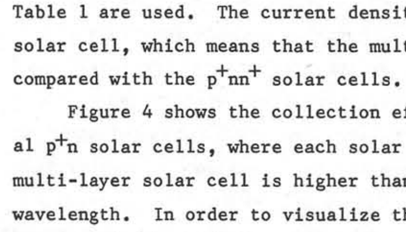

Figure 2

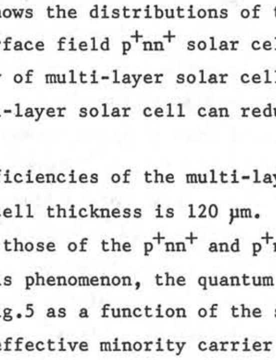

Figure 3

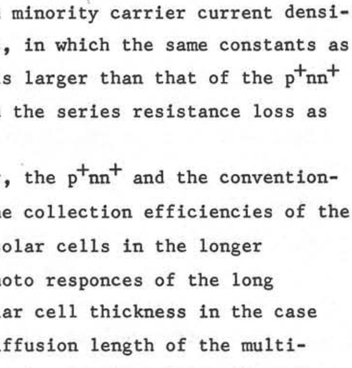

Figure 4

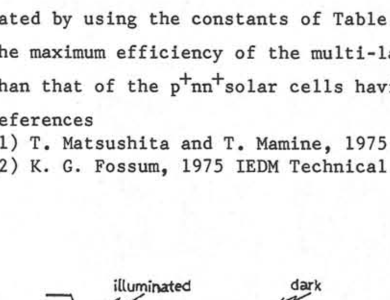

Figure 5

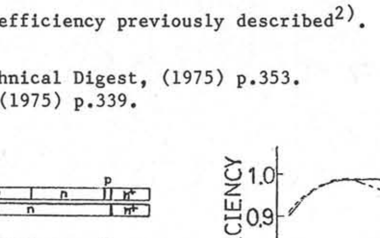

Figure 6